JURNAL KIMIA VALENSI
p-ISSN: 2460-6065; e-ISSN: 2548-3013
Journal homepage: https://journal.uinjkt.ac.id/index.php/valensi
Research Article

Modified Bacterial Cellulose-Based Composite Profile for Drug Release of Tetracycline Hydrochloride

Ni Wayan Chyntia Pramesti Cahyani[1], Emmy Yuanita[1], Ni Komang Tri Dharmayani[1], Sudirman[1], Ni Made Sudewianingsih[2], Maria Ulfa[1*]

[1]*Chemistry Department, Faculty of Mathematics and Natural Science, University of Mataram, Mataram-NTB, 83125 Indonesia*
[2]*Biology Laboratory, Faculty of Mathematics and Natural Science, University of Mataram, Mataram-NTB, 83125 Indonesia*

Email: ulfaarief@unram.ac.id

Article Info
Received: Feb 13, 2024
Revised: Feb 23, 2024
Accepted: April 19, 2024
Online: June 09, 2024

Citation:
Cahyani, N. W. C. P., Yuanita, E., Dharmayani, N. K. T., Sudirman, Sudewianingsih, N. M., & Ulfa, M. (2024). Modified Bacterial Cellulose-Based Composite Profile for Drug Release of Tetracycline Hydrochloride. *Jurnal Kimia Valensi*, *10*(1), 76 - 85.

Doi: 10.15408/jkv.v10i1.37663

Abstract
Bacterial cellulose (BC) is a biodegradable natural polymer with high mechanical strength and non-toxicity. This biopolymer is widely used as a candidate in biomedical fields, such as drug delivery, wound healing, and filtration systems. However, BC lacks antibacterial activity which limits its use in biomedical applications. So, modification of BC-based composite is required. This study aims to examine the effects of modifying BC-based composites with fillers such as graphite (G) and polyvinyl alcohol (PVA) on the release of tetracycline hydrochloride (TCH) drugs. Adding fillers to BC can alter its physical and mechanical properties, reducing its porosity and swelling rate in acidic and alkaline mediums. The drug release of TCH from modified BC-based composites follows the Korsmeyer-Peppas and Hixson-Crowell kinetics models. Adding filler and TCH antibiotic to the composite enhances its antibacterial activity against *Staphylococcus aureus* with a significant inhibition zone. The results of the inhibition zone show that composites have the potential to be applied in biomedical fields, especially in transdermal patches.

Keywords: Bacterial cellulose; graphite; drug release; polyvinyl alcohol; tetracycline hydrochloride

1. INTRODUCTION

Drug release is the process of transferring drug solute from a material medium to the release medium [1]. To ensure effective drug releases, factors such as drug loading ratio and controlled release rate are crucial [2]. The main challenge lies in selecting a safe, non-toxic, and eco-friendly material that can maintain good biological activity. Controlled drug-release systems can use various materials, including polymers, where the drug-release rate depends on the matrix's structure and properties [3]. The release of drugs with polymer-based can be achieved by forming a composite. Composite is a combination of two or more materials that exhibit desirable properties due to the combination of constituent materials used.

Natural polymers like cellulose, starch, and glycogen have been researched for their potential in drug release applications [4]. Studies have shown cellulose-based materials, especially bacterial cellulose (BC), have several benefits in biomedical fields, including drug release [5]. Bacterial cellulose is a biodegradable natural polymer with high mechanical strength, biocompatibility, and non-toxicity. It has a high-water content (98-99%) and can be sterilized without affecting its properties. However, BC lacks antibacterial activity, which limits its use in biomedical applications. Therefore, in-situ or ex-situ modification of BC-based composites is necessary [6]. BC-based composites can be created by filling the porous BC matrix with particle solutions or suspensions through physical absorption.

BC-based composites have demonstrated effective antibacterial activity, which can be further enhanced by incorporating inorganic and organic antibacterial agents and antibiotics [6]. Research has shown that BC/G composites, which combine BC with graphite, exhibit high biocompatibility and improved mechanical properties while also providing mechanical inhibitory

properties against bacterial growth by damaging bacterial cell membranes when exposed to graphite sheets [7,8]. However, the non-homogeneous distribution of graphite within the composite matrix and weak interfacial bonding between graphite and the matrix are crucial challenges to obtaining such functional composites for the biomedical field [9]. Furthermore, BC/PVA composites, created by combining BC with PVA, have been synthesized and found to have small molecular permeability, low interfacial tension, and the ability to release antibiotics in a controlled manner [10]. PVA also enhances the adhesion of BC and improves the interaction between the matrix and filler, making the filler distribution in the polymer matrix homogeneous and strengthening the mechanical effect of inhibiting bacterial growth [11,12]. However, PVA has weak mechanical properties [13].

It has been found that the antibacterial properties of BC-based composites can be enhanced by incorporating antibiotics. Tetracycline hydrochloride (TCH) is an antibiotic that can target gram-negative and gram-positive bacteria and possesses a controlled drug release profile [14].

Considering this, the novelty of this research lies in modifying BC-based composites with additional G and PVA fillers. The antibiotic TCH incorporated into the composite determines the drug release profile and kinetics. The addition of fillers graphite and PVA is expected to be a promising combination to obtain materials suitable for biomedical applications. Since drug release depends on many factors, this paper formulates a good drug release profile of TCH in BC/G/PVA composites using mathematical models including zero-order, first-order, Higuchi, Hixon-Crowell, and Korsmeyer- Peppas [15]. Antibacterial activity testing was conducted against *S. aureus* to observe its antibacterial performance when applied in the biomedical field.

2. RESEARCH METHODS

Materials

The research materials used in this study include BC (UMKM Yogyakarta, FarahShop), graphite (Merck), polyvinyl alcohol (Merck), potassium persulfate (Sigma-Aldrich), sodium hydroxide (Merck), n-butanol 80% v/v (Sigma-Aldrich), tetracycline hydrochloride (Merck), Cetyl trimethyl ammonium bromide (CTAB) (Merck), methanol 96% v/v (Merck), and buffer solutions with pH 1.2 to 8.4 (Sigma-Aldrich).

Equipment/Instruments

The research tools used in this research include standard laboratory glassware, a hot plate stirrer (IKA C-MAG HS 7), oven (Memmert), ultrasonication (Trias Nathomi Chemindo), furnace (ThermoScientific), analytical balance (Fujitsu), pH meter (RoHS), and digital screw micrometer (T&E CR1632). The instruments used in this research include the FTIR instrument (PerkinElmer), SEM-EDS instrument (JEOL JCM-7000), UV-Vis spectrophotometer instrument (Thermofisher), and tensilon (RTG-1310).

Purification of Bacterial Cellulose (BC)

Purification was achieved by repeatedly washing BC with hot water and cooling it. The resulting material was soaked in 0.5 M NaOH for 24 hours and rinsed with distilled water until the pH reached 7 [16].

Composite Fabrication

Based on a previous method with modifications, graphite (0.5% w/v) was calcined (1000 ˚C, 5 min) and then homogenized using ultrasonication for 7 hours with the addition of CTAB (0.3% w/v) as a surfactant [7]. The BC hydrogel was added to the graphite solution, which had a known moisture content and weight, and homogenized by ultrasonication for 6 hours. Next, the composite with reduced water content was reacted in a PVA solution (0.03 wt%), to which a $K_2S_2O_8$ initiator (0.04 wt%) was added and homogenized by ultrasonication at 55 ˚C for 3 hours. The selection of potassium persulfate as the initiator is because of its solubility in water and aims to trigger polymerization. The monomer will react with the initiator to form free radicals in the solution system, followed by the reaction between monomers to form homopolymers [17]. Finally, the obtained composite was dried for two days at 25 ˚C [12]. The illustration for fabrication of composite is presented in **Figure 1**.

Characterization

SEM-EDS Analysis

The JEOL SEM-EDS instrument was utilized to analyze the morphology and atomic composition of the composite at the integrated laboratory of the State Islamic University of Mataram, Indonesia. Operating condition EDS was landing at an acceleration voltage of 15 kV, working distance of 12.7 mm, magnification ×2,000, and vacuum mode high.

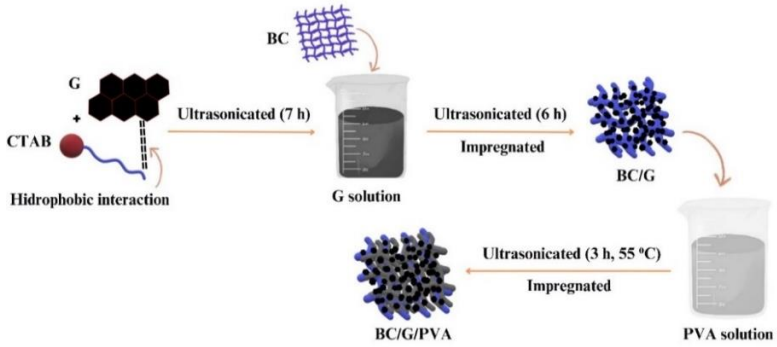

Figure 1. Schematic representation of a method for fabrication of BC/G/PVA composite

Fourier Transform Infra-Red (FTIR) Analysis

The functional groups of the composite structure were analyzed using FTIR (Perkin-Elmer) at the integrated laboratory of the State Islamic University of Mataram, Indonesia. Sample configured with Attenuated Total Reflection FTIR (ATR-FTIR) at room temperature and carried out at wave numbers 4000 to 500 cm^{-1} with a scanning resolution of 2 cm^{-1}.

Physical and Mechanical Characterization

Physical characterization included thickness and porosity tests. Thickness measurements were taken at ten different points in each sample using a digital screw micrometer (T&E CR1632) and calculated with equation 1 [18].

$$\dot{t} = \frac{t_1+t_2+\ldots t_n}{n} \quad (1)$$

The value of t represents the thickness (in 10^{-3} cm), n represents the number of data, and $\dot{t}$ represents the average thickness (in 10^{-3} cm). Porosity was measured by immersing the sample in 80% v/v n-butanol and then calculated using equation 2 [19].

$$\phi = \frac{(Mb-Mk)}{\rho B \times Vk} \times 100\ \% \quad (2)$$

The value of ϕ is porosity (%), Mk is the dry mass of the sample (g), Mb is the wet mass of the sample (g), ρB is the density of n-butanol (g/cm³), Vk is the dry volume of the sample (cm³). Mechanical characterization includes tensile strength and young modulus. A tensile strength test was conducted using a tension tool (RTG-1310). The tensile strength can be calculated based on equation 3 [20].

$$\sigma_t = \frac{F_t}{A_t} \quad (3)$$

The value σt is the tensile strength (MPa), Ft is the maximum stress (N), and A_t is the cross-sectional area of the composite subjected to stress (mm^2).

Swelling Rate

The swelling ratio was evaluated by immersing the weighed and dried samples at room temperature until reached equilibrium and calculate using equation 4 [20].

$$WAC = \frac{(Ws-Wd)}{Wd} \times 100\ \% \quad (4)$$

Ws is the wet sample weight, Wd is the dry sample weight, and WAC is the swelling ratio.

Drug Release Kinetics

The assay was carried out in pH 6.86 medium (4 hours) at 30-minute intervals and analyzed using a UV-Vis spectrophotometer (Thermofisher) at the maximum wavelength of TCH. The data obtained were fitted to the kinetic model using equations 5, 6, 7, 8, and 9, representing zero-order, first-order, Higuchi, Hixson-Crowell, and Korsmeyer-Peppas, respectively [15].

$$Q = kt \quad (5)$$

$$\log Q = \frac{kt}{2.303} \quad (6)$$

$$Q = kt^{1/2} \quad (7)$$

$$\left(1 - \frac{M_t}{M_\infty}\right)^{\frac{1}{3}} = -kt \quad (8)$$

$$\frac{M_t}{M_\infty} = kt^n \quad (9)$$

The Q value is the concentration of the drug released, k is the drug release rate constant, t is the drug release time, M_t/M_∞ is the fractional release of the drug, and n is the diffusion exponent.

Antibacterial Activity

The study tested the effectiveness of a composite material in killing *S. aureus* bacteria using the disc diffusion method. The Advanced Biology Laboratory at FMIPA University of Mataram provided the bacterial strains. The composite was applied onto the media containing the bacterial strains and incubated for 24 hours at 37 ˚C. The diameter of the zone where the composite inhibited the growth of *S. aureus* was then measured.

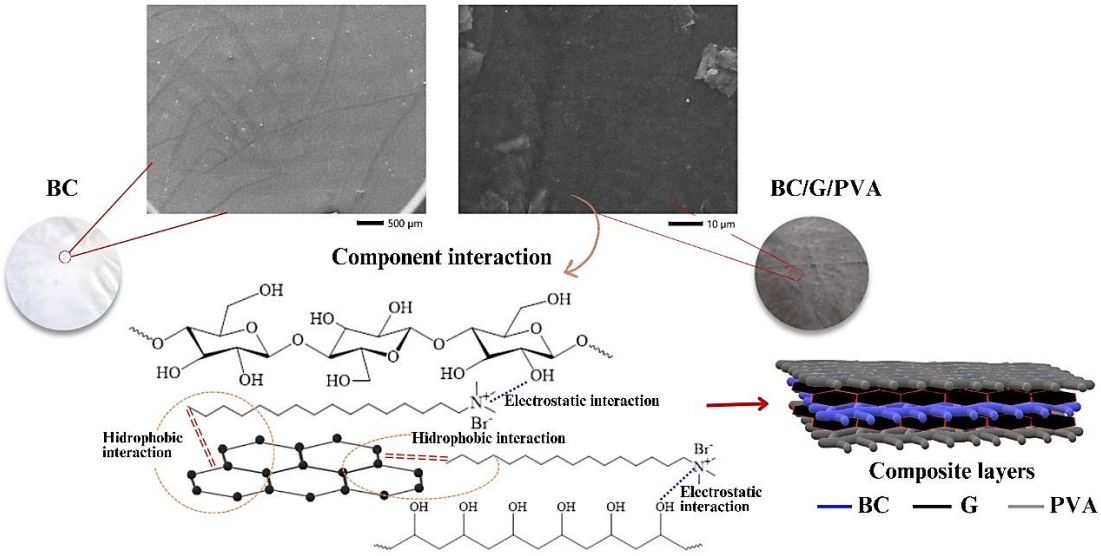

Figure 2. Illustration of graphite and PVA filler in BC matrix

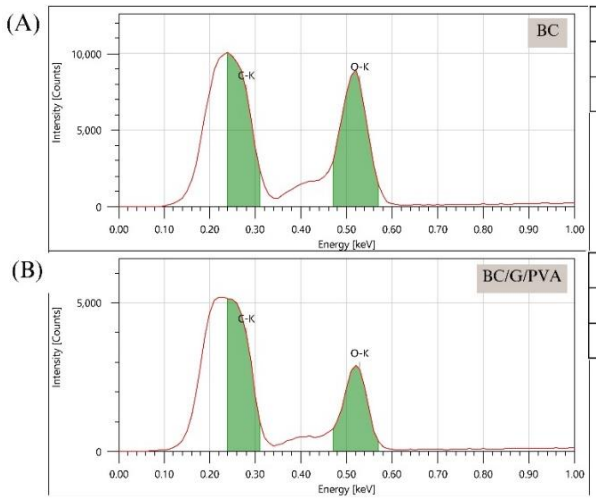

Element	Mass %	Atom %
C-K	32.94 ± 0.33	39.55 ± 0.40
O-K	67.06 ± 0.87	60.45 ± 0.78

Element	Mass %	Atom %
C-K	36.35 ± 0.54	43.20 ± 0.64
O-K	63.65 ± 1.38	56.80 ± 1.23

Figure 3. EDS spectra of (A) BC; (B) BC/G/PVA

3. RESULTS AND DISCUSSION

Morphology and Chemical Analysis of Composite Film

According to **Figure 2**, the morphology of pure BC is smoother and flatter than that of BC/G/PVA. The darker color in BC/G/PVA indicates the presence of G and PVA absorbed in BC. Similar research was experienced during the synthesis of BC-based composite with the addition the chitosan, resulting in a grey coloration. This is caused by the presence of chitosan during the composite synthesis process [21]. Graphite is characterized by flat flakes with sharp corners, while PVA appears evenly dispersed in the composite [22,23]. The interactions between G and PVA fillers in the BC matrix are attributed to hydrophobic and electrostatic interactions with CTAB as a surfactant. CTAB is a cationic surfactant with an ammonium (N^+) head group and a hydrophobic alkyl chain tail composed of cetyl groups [7]. Hydrophobic interactions occur between the alkyl tails of CTAB and G. In contrast, electrostatic interactions occur between hydroxy groups on BC and PVA with quaternary ammonium groups (N^+) on CTAB, which are hydrophilic [24]. The presence of CTAB can reduce the hydrophobic nature of G, allowing it to spread in the BC matrix.

According to the EDS test results shown in **Figure 3**, the composition of the BC/G/PVA composite is the same as that of pure BC but with different masses and atomic compositions. The increase in the number of C atoms in BC/G/PVA is due to the addition of filler G and PVA, which are absorbed into the cellulose fibers during ultrasonication. A similar effect was observed in a previous study when researchers added G to the BC matrix [7]. The addition of G and PVA can reduce the composition of O atoms, which is reflected in the molecular formula of each component: BC ($C_6H_{10}O_5$), G (consisting mainly of C atoms), and PVA (C_2H_4O). Comparing the elements in each component reveals that the number of C atoms is significantly higher than that of O atoms. Similar research was experienced during the

synthesis of BC/PVA and BC/PVA/TiO_2, resulting in the differences in composition of O atoms which were not much different, only 0.1% before and after the addition of TiO_2 [23].

Identification of Functional Groups of Composite Film

The FTIR spectra demonstrate that all BC, G, and PVA characteristic bands overlap. Although the FTIR spectra in **Figure 4** do not show any addition of new functional groups, there is a shift towards lower wave numbers in the strain vibration peak and a change in the intensity of the C-O-C absorption band in the BC/G/PVA composite. This shift and change in intensity are due to the interaction between each composite component, shown in **Figure 2**. The results obtained indicate that the interactions that occur are only physical interactions [20,25].

The absorption bands at 3342 and 3338 cm^{-1} suggest the presence of O-H stretching, supported by the absorption bands at 1324 and 1322 $cm^{-1,}$ indicating the presence of C-O. These bands are also characteristic of BC and acetyl groups in PVA [20,26,27]. The absorption bands at 2914 and 2900 cm^{-1} confirm the presence of C-H stretching, reinforced by C-H bending at 1442 and 1437 cm^{-1}. The C-O-C absorption band, which indicates the antisymmetric stretching of 1,4-β-D-glucoside in BC, has a broader intensity and shifts to a lower wave number in BC/G/PVA, possibly due to C-O-H vibrations. This effect could be attributed to the addition of PVA, as supported by research by Vo et al. (2019), during FTIR characterization of PVA, C-O-H vibrations were observed around the wave number 1090 cm^{-1} [28].

Physical and Mechanical Properties

Table 1 shows that the thickness of the composite increased with the addition of G and PVA fillers. Filler added as a modifying agent has an impact on the composite thickness. Fillers increase the composite density, which can fill the cavities in the BC fiber. However, as the filler increases, the porosity of the composite decreases [29]. These results were obtained from Tanpichai et al. (2019) research, where cellulose nanofibrils as fillers increased the composite thickness and reduced its porosity [30]. The PVA has a biocompatible ability to form films, which can be used as a composite binder to minimize pores and increase composite density [11].

It was discovered that the tensile strength of the composite decreased as the filler increased. This opposes previous research that suggested adding PVA to the cellulose matrix would increase the tensile strength value of the composite [28]. The decrease in tensile strength value is due to an increase in filler load caused by a reduction in matrix cross-section and an increase in stress concentration [29]. Adding G to the composite can similarly decrease the tensile strength value by adding

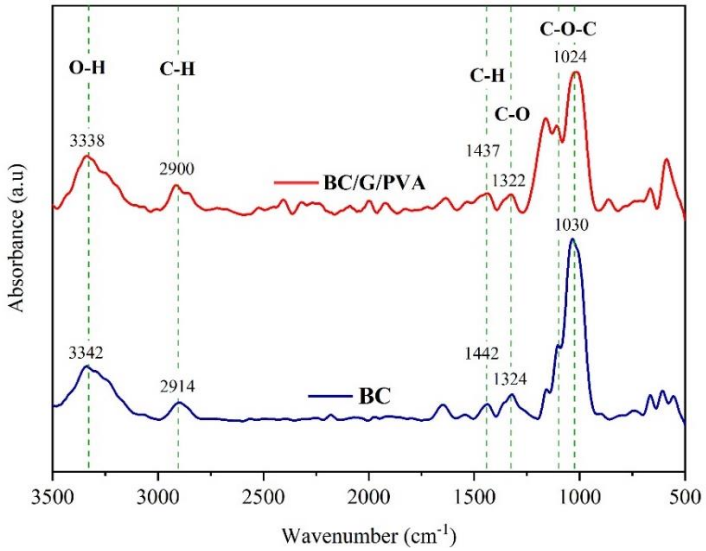

Figure 4. FTIR spectra of BC and BC/G/PVA

Table 1. Physical and mechanical properties of composite

Composite	Characterization		
	Thickness (10^{-3} cm)	Porosity (%)	Tensile Strength (MPa)
BC	4.370 ± 0.240	52.783 ± 4.798	60.054
BC/G/PVA	8.890 ± 0.210	14.152 ± 3.538	4.299

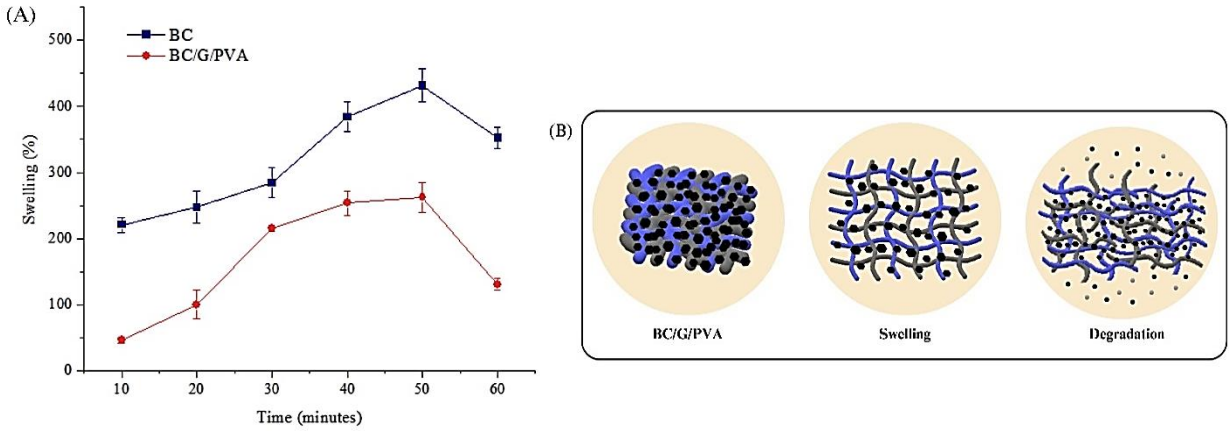

Figure 5. (A) Swelling graph with time variation; (B) Schematic representation of the swelling process BC/G/PVA composite

surfactant in the form of CTAB while fabricating BC/G composites. A similar reduction in tensile strength value was observed by another researcher who obtained a value of 68 MPa due to the addition of CTAB to the BC/G composite. The presence of CTAB leads to a low number of O-H bonds because the hydrophilic CTAB head interacts with O-H groups on BC and PVA, thus negatively affecting the tensile strength value of the composite [19].

Swelling Rate

The results of the swelling test, shown in **Figure 5A**, demonstrate that adding filler to a composite reduces its swelling ratio. This is due to the low porosity of the composite, which makes it difficult for water to fill the cavities, thus decreasing the swelling ratio [29]. The size of the swelling value is an essential parameter for drug release [21]. The composite reached its maximum swelling state at 50 minutes. It began to experience a decrease in the swelling ratio at 60 minutes due to environmental exposure or mechanical stress, which can cause degradation of the composite. Degradation can occur due to breaking glycosidic bonds in BC during hydrolysis [12,31]. This is characterized by dissolved graphite and PVA particles, leaving parts of BC uncoated with fillers, leading to degradation. However, this degradation can be an advantage in the biomedical field [32], such as drug release. An illustration of composite degradation is presented in **Figure 5B**.

Figure 6 presents the swelling ratio of a composite material at different pH levels. The results show that the composite is sensitive to pH changes, with the highest swelling ratio occurring at pH 7.4 and the lowest at pH 1.2. The hydrophilic nature of PVA is affected by ionization caused by acidic or alkaline pH levels, as PVA has a hydroxyl group (-OH) that can be ionized. PVA is neutral at a pH of 7.4, making it more hydrophilic. The swelling ratio can be used to determine the suitability of drug release in specific organs. The maximum PVA filler composite with dexamethasone drug was released at pH 6.8-7.4, which is compatible with intestinal fluids [31].

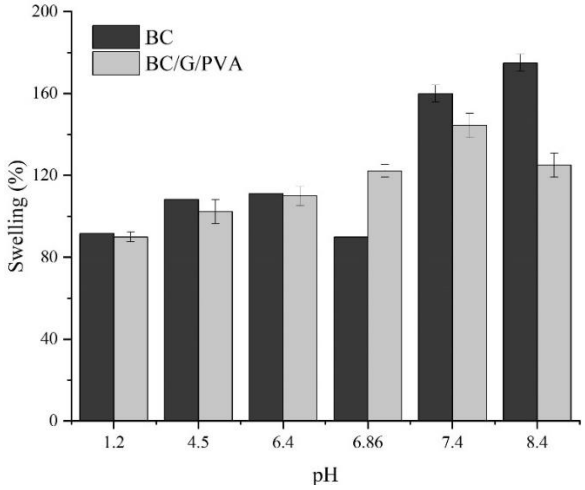

Figure 6. Swelling graph with pH variation

Drug Release Profile of Composite

According to **Figure 7**, the different drug release rates in the composites during the first and second stages are due to the formation of drug-polymer structural units of various sizes [15]. The porosity of the composite can have an impact on the adsorption and release of TCH drugs. The release of TCH drugs is also influenced by the competition between the affinity of TCH for the adsorbent surface and its solubility in the release medium [33]. This mathematical drug release model has different regression coefficient (R^2) values in the release medium of pH 6.86, shown in **Table 2**. The R^2 value is the most reliable way to describe the drug release profile of a composite [12].

Table 2 shows BC has drug release in the first and second stages following a zero-order kinetics model. The R^2 values for the two stages are 0.9609 and 1, respectively. Zero-order drug release means that the release does not depend on the concentration of the drug

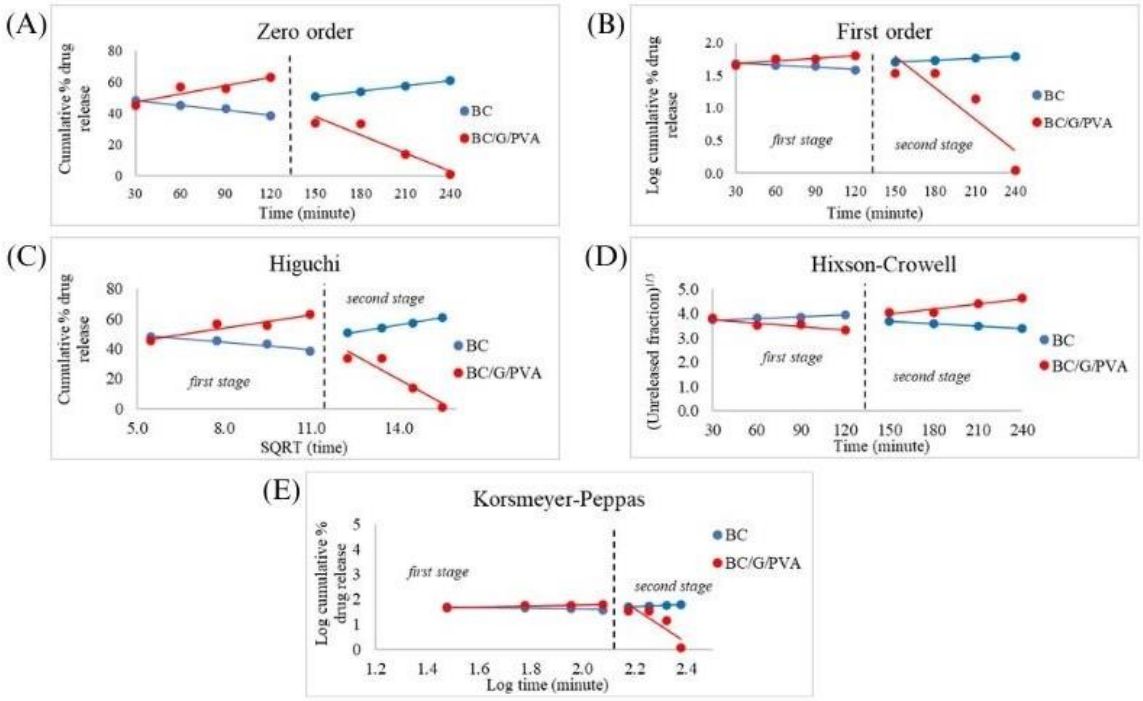

Figure 7. Linear models of drug release profile (A) Zero-order; (B) First-order; (C) Higuchi; (D) Hixson-Crowell; (E) Korsmeyer-Peppas

Table 2. Drug release profile based on different models at pH 6.86

Model Code	Zero-Order		First-Order		Higuchi		Hixson-Crowell		Korsmeyer-Peppas	
	K (10^{-2})	R^2	K (10^{-2})	R^2	K (10^{-2})	R^2	K (10^{-2})	R^2	K (10^{-2})	R^2
BC*	10.387	0.9609	0.105	0.9480	167.369	0.9246	0.234	0.9566	14.747	0.8491
BC/G/PVA*	17.52	0.8389	0.142	0.8241	293.046	0.8697	0.459	0.8486	21.88	0.8925
BC**	0.113	1	8.911	0.9992	3.158	0.9987	0.304	0.9995	0.392	0.9982
BC/G/PVA**	39.18	0.8873	1.611	0.7947	10.768	0.8873	0.699	0.9039	683.34	0.7367

*1st stage **2nd stage

in the delivery system [34]. The high porosity of BC allows the entry of fillers and medicines, which can affect the release kinetics model of these substances [6].

Drug release of TCH on BC/G/PVA composite followed the Korsmeyer-Peppas kinetics model in the first stage (30 to 120 minutes) and the Hixson-Crowell model in the second stage (150 to 240 minutes). The R^2 values for the two stages are 0.8925 and 0.9039, respectively. The Hixson-Crowell model indicates that the mechanism of drug release from the composite is influenced by its surface area, and the dissolution rate of the drug particles affects the drug release. The addition of fillers G and PVA caused a compact composite structure with small pore sizes. So that facilitating slow and controlled drug release. The biomedical effectiveness of the Hixon-Crowell kinetic model enables to absorb and release of drugs for application in transdermal patches [21].

Furthermore, drug release at the first stage plotted with the Korsmeyer-Peppas model tends to experience a diffusion process, with a linear regression equation of y = 0.2189x + 1.3406. The diffusion exponent (n) value is 0.2189, indicating that the diffusion mechanism of the composite includes Quasi-Fickian diffusion because n is less than 0.5 [35]. Quasi-Fickian diffusion, like Fickian diffusion, describes drug release depending on polymer relaxation and material degradation [36].

Antibacterial Activity of Composite

The antibacterial properties of a composite material can be measured by determining the zone of bacterial inhibition against the composite. **Figure 8** shows that BC and BC/G/PVA composites have different inhibition zones against *S. aureus*. Adding filler G and PVA can enhance the antibacterial activity of BC-based composites. Graphite's sharp edges can break the bacterial membrane, providing mechanical inhibition. Part of the composite will interact with the bacterial membrane, consisting of lipopolysaccharides and phospholipids, thus penetrating several functional groups in bacteria to inhibit bacterial growth [12]. Adding G and PVA can also improve the matrix's interaction and

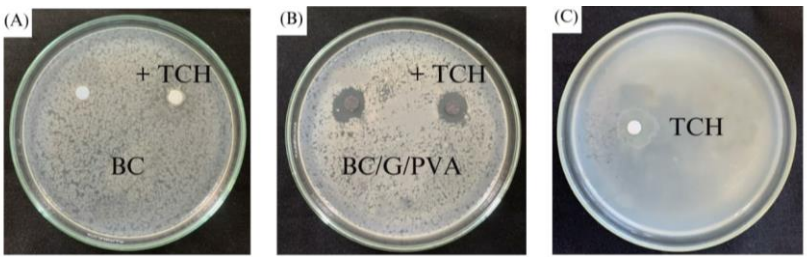

Figure 8. Antibacterial activity of (A) BC; (B) BC/G/PVA; (C) Control TCH

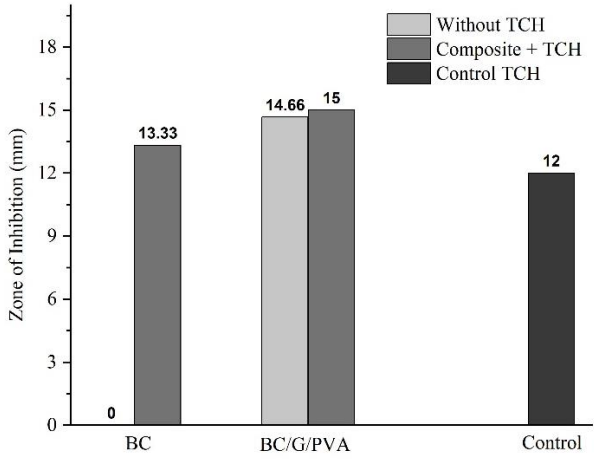

Figure 9. Inhibition zone graph of composite against *S. aureus*

dispersion of antibacterial agents, allowing for better contact between the antibacterial agent and bacteria. This results in increased antibacterial effectiveness of the composite [37].

Adding antibiotics can help to identify signs of bacterial resistance to composite [21]. **Figure 9** shows that adding antibiotics to BC and BC/G/PVA led to higher bacteria inhibition than before the addition and the TCH-positive control. BC-based composites with G and PVA fillers, as well as antibiotics, have the potential to be antibacterial membranes with an average inhibition zone of 15 mm.

4. CONCLUSION

The BC/G/PVA composite has been successfully synthesized, and the drug release of TCH on the composite followed the Korsmeyer-Peppas kinetics model in the first stage and Hixson-Crowell in the second stage. Adding filler G and PVA increased the composite's cohesiveness, making it suitable for use as a drug-release formulation material. Furthermore, adding fillers and antibiotics increased the composite's antibacterial activity against *S. aureus*. The composite has shown an average inhibition zone of 15 mm, indicating that it has the potential to be used in the field of biomedicine.

ACKNOWLEDGMENTS

This project was carried out with the support of DIPA BLU funds for the University of Mataram's capacity-building research scheme under contract number 1423/UN18.L1/PP/2023. We want to express our gratitude to all parties involved, particularly the Basic Physics Laboratory of Mataram University staff and the Integrated Laboratory of UIN Mataram.

REFERENCES

1. Sharma K, Porat Z, Gedanken A. Designing natural polymer-based capsules and spheres for biomedical applications—A review. *Polymers (Basel)*. 2021;13(24):1-41. doi:10.3390/polym13244307
2. Li X, Liu Y, Yu Y, Chen W, Liu Y, Yu H. Nanoformulations of quercetin and cellulose nanofibers as healthcare supplements with sustained antioxidant activity. *Carbohydr Polym*. 2019;207:160-168. doi:10.1016/j.carbpol.2018.11.084
3. Adepu S, Ramakrishna S. Controlled drug delivery systems: current status and future directions. *Molecules*. 2021;26(19):1-45. doi:doi: 10.3390/molecules26195905
4. Srivastava N, Richa, Roy Choudhury A. Recent advances in composite hydrogels prepared solely from polysaccharides. *Colloids Surf B Biointerfaces*. 2021;205:1-15. doi:10.1016/j.colsurfb.2021.111891
5. Stumpf TR, Yang X, Zhang J, Cao X. In situ and ex situ modifications of bacterial cellulose for applications in tissue engineering. *Materials Science and Engineering C*. 2018;82:372-383. doi:10.1016/j.msec.2016.11.121

6. Zheng L, Li S, Luo J, Wang X. Latest advances on bacterial cellulose-based antibacterial materials as wound dressings. *Front Bioeng Biotechnol*. 2020;8:1-15. doi:10.3389/fbioe.2020.593768
7. Aritonang HF, Wulandari R, Wuntu AD. Synthesis and characterization of bacterial cellulose/nano-graphite nanocomposite membranes. *Macromol Symp*. 2020;391(1):1-7. doi:10.1002/masy.201900145
8. Liauw CM, Vaidya M, Slate AJ, et al. Analysis of cellular damage resulting from exposure of bacteria to graphene oxide and hybrids using fourier transform infrared spectroscopy. *Antibiotics*. 2023;12(4):1-20. doi:10.3390/antibiotics12040776
9. Silva M, Alves NM, Paiva MC. Graphene-polymer nanocomposites for biomedical applications. *Polym Adv Technol*. 2018;29(2):687-700. doi:10.1002/pat.4164
10. Song S, Liu Z, Abubaker MA, et al. Antibacterial polyvinyl alcohol/bacterial cellulose/nano-silver hydrogels that effectively promote wound healing. *Materials Science and Engineering C*. 2021;126:1-13. doi:10.1016/j.msec.2021.112171
11. Tai MH, Mohan BC, Yao Z, Wang CH. Superhydrophobic leached carbon black/poly(vinyl) alcohol aerogel for selective removal of oils and organic compounds from water. *Chemosphere*. 2022;286:1-10. doi:10.1016/j.chemosphere.2021.131520
12. Al-Arjan WS, Khan MUA, Almutairi HH, Alharbi SM, Razak SIA. pH-Responsive PVA/BC-f-GO dressing materials for burn and chronic wound healing with curcumin release kinetics. *Polymers (Basel)*. 2022;14(10):1-16. doi:10.3390/polym14101949
13. Tan BK, Ching YC, Poh SC, Abdullah LC, Gan SN. A review of natural fiber reinforced poly(vinyl alcohol) based composites: Application and opportunity. *Polymers (Basel)*. 2015;7(11):2205-2222. doi:10.3390/polym7111509
14. Shao W, Liu H, Wang S, et al. Controlled release and antibacterial activity of tetracycline hydrochloride-loaded bacterial cellulose composite membranes. *Carbohydr Polym*. 2016;145:114-120. doi:10.1016/j.carbpol.2016.02.065
15. Iftime MM, Dobreci DL, Irimiciuc SA, Agop M, Petrescu T, Doroftei B. A theoretical mathematical model for assessing diclofenac release from chitosan-based formulations. *Drug Deliv*. 2020;27(1):1125-1133. doi:10.1080/10717544.2020.1797242
16. Syamsu K, Kuryani DT. Pembuatan Biofilm Selulosa Asetat dari Selulosa Mikrobial Nata De Cassava. *Jurnal Agroindustri Indonesia* . 2014;3(1):126-133. http://tin.fateta.ipb.ac.id/journal/e-jaii
17. Sari TI, Hadiah F, Bahrin D, Putri TJ, Amanda R. Pengaruh konsentrasi inisiator kalium persulfat dan monomer asam akrilat terhadap persen grafting karet alam/starch. *Jurnal Teknik Kimia*. 2023;29(1):9-18. doi:10.36706/jtk.v29i1.1450
18. Galdino CJS, Maia AD, Meira HM, et al. Use of a bacterial cellulose filter for the removal of oil from wastewater. *Process Biochemistry*. 2020;91:288-296. doi:10.1016/j.procbio.2019.12.020
19. Xu K, Qin Y, Xu T, et al. Combining polymeric membranes with inorganic woven fabric: Towards the continuous and affordable fabrication of a multifunctional separator for lithium-ion battery. *J Memb Sci*. 2019;592:1-9. doi:10.1016/j.memsci.2019.117364
20. Dewi R, Sylvia N, Riza M. Characterization of Degradable Plastics from Sago and Breadfruit Starch-Based with Addition of Zinc Oxide (ZnO) Catalyst and Polyvinyl Alcohol (PVA). *Jurnal Kimia Sains dan Aplikasi*. 2023;26(11):427-436. doi:10.14710/jksa.26.11.427-436
21. Arikibe JE, Lata R, Rohindra D. Bacterial Cellulose/Chitosan Hydrogels Synthesized In situ for Biomedical Application. *J Appl Biosci*. 2021;162:16675-16693. doi:10.35759/jabs.162.1
22. Susilo BD, Suryanto H, Aminnudin A. Characterization of bacterial nanocellulose - graphite nanoplatelets composite films. *Journal of Mechanical Engineering Science and Technology*. 2021;5(2):145. doi:10.17977/um016v5i22021p145
23. Sharma D, Kumari M, Dhayal V. Fabrication and characterization of cellulose/pva/tio2 nanocomposite thin film as a photocatalyst. *Mater Today Proc*. 2021;43:2970-2974. doi:10.1016/j.matpr.2021.01.323
24. Arfi R Ben, Karoui S, Mougin K, Ghorbal A. Cetyltrimethylammonium bromide-treated Phragmites australis powder as novel polymeric adsorbent for hazardous Eriochrome Black T removal from aqueous solutions. *Polymer Bulletin*. 2019;76(10):5077-5102. doi:10.1007/s00289-018-2648-8
25. Fuller ME, Andaya C, McClay K. Evaluation of ATR-FTIR for analysis of bacterial cellulose impurities. *J Microbiol Methods*. 2018;144:145-151. doi:10.1016/j.mimet.2017.10.017
26. Khalid A, Ullah H, Ul-Islam M, et al. Bacterial cellulose-TiO2 nanocomposites promote healing and tissue regeneration in burn mice model. *RSC Adv*. 2017;7(75):47662-47668. doi:10.1039/c7ra06699f

27. Ulfa M, Noviani I, Yuanita E, Dharmayani NKT, Sudirman, Sarkono. Synthesis and Characterization of Composites-Based Bacterial Cellulose by Ex-Situ Method as Separator Battery. *Jurnal Penelitian Pendidikan IPA*. 2023;9(6):4647-4651. doi:10.29303/jppipa.v9i6.3819
28. Vo TV, Dang TH, Chen BH. Synthesis of intelligent pH indicative films from chitosan/poly(vinyl alcohol)/anthocyanin extracted from red cabbage. *Polymers (Basel)*. 2019;11(7). doi:10.3390/polym11071088
29. Nuryati, Amalia RR, Hairiyah N, et al. Pembuatan komposit dari limbah plastik polyethylene terephthalate (PET) berbasis serat alam daun pandan laut (Pandanus tectorius). *Agroindustri*. 2020;10(2):107-117. doi:10.31186/j.agroind.10.2.107-117
30. Tanpichai S, Witayakran S, Srimarut Y, Woraprayote W, Malila Y. Porosity, density and mechanical properties of the paper of steam exploded bamboo microfibers controlled by nanofibrillated cellulose. *Journal of Materials Research and Technology*. 2019;8(4):3612-3622. doi:10.1016/j.jmrt.2019.05.024
31. Rizwan M, Yahya R, Hassan A, et al. pH sensitive hydrogels in drug delivery: brief history, properties, swelling, and release mechanism, material selection and applications. *Polymers (Basel)*. 2017;9(4):1-37. doi:10.3390/polym9040137
32. Rohaeti E, LFX EW, Rakhmawati A. Kemudahan Biodegradasi Selulosa Bakteri dari Limbah Cucian Beras dengan Penambahan Gliserol, Kitosan, dan Nanopartikel Perak. *Jurnal Kimia Valensi*. 2016;2(1):45-54. doi:10.15408/jkv.v2i1.3111
33. Ananda MB. Mesoporous Silica Nanoparticles Sebagai Drug Carrier pada Aplikasi Controlled Drug Delivery System. *Jurnal Perancangan, Manufaktur, Material, dan Energi (Jurnal Permadi)*. 2020;2(3):102-109. doi:10.52005/permadi.v2i3.39
34. Jantarat C, Muenraya P, Srivaro S, Nawakitrangsan A, Promsornpason K. Comparison of drug release behavior of bacterial cellulose loaded with ibuprofen and propranolol hydrochloride. *RSC Adv*. 2021;11(59):37354-37365. doi:10.1039/d1ra07761a
35. Paarakh MP, Jose PA, Setty C, Christoper GVP. *Release Kinetics-Concepts And Applications*.; 2018. https://www.researchgate.net/publication/369038187
36. Bayer IS. Controlled drug release from nanoengineered polysaccharides. *Pharmaceutics*. 2023;15(5):1-43. doi:10.3390/pharmaceutics15051364
37. Hajeeassa KS, Hussein MA, Anwar Y, Tashkandi NY, Al-Amshany ZM. Nanocomposites containing polyvinyl alcohol and reinforced carbon-based nanofiller: A super effective biologically active material. *Nanobiomedicine (Rij)*. 2018;5:1-12. doi:10.1177/1849543518794818